EUROPHYSICS LETTERS

Europhys. Lett. (2006)

DOI: `10.1209/epl/i2005-10494-2`

Nuclear resonant forward scattering of synchrotron radiation from ^{121}Sb at 37.13 keV

H.-C. Wille[1], Yu. V. Shvyd'ko[2], E. E. Alp[2], H. D. Rüter[3], O. Leupold[4], I. Sergueev[1], R. Rüffer[1], A. Barla[5] and J. P. Sanchez[6]

[1] *European Synchrotron Radiation Facility - F-38043 Grenoble Cedex, France*
[2] *Argonne National Laboratory, Advanced Photon Source - Argonne, IL 60439, USA*
[3] *Institut für Experimentalphysik, Universität Hamburg - D-22761 Hamburg, Germany*
[4] *Hamburger Synchrotronstrahlungslabor - D-22607 Hamburg, Germany*
[5] *IPCMS/GEMME - F-67034 Strasbourg Cedex 2, France*
[6] *CEA Grenoble - F-38054 Grenoble Cedex 9, France*

received 13 September 2005; accepted in final form 2 February 2006

PACS. `76.80.+y` – Mössbauer effect; other gamma-ray spectroscopy.
PACS. `41.85.Si` – Beam collimators, monochromators.
PACS. `29.20.Lq` – Synchrotrons.

Abstract. – We report on the observation of nuclear resonant forward scattering of synchrotron radiation from ^{121}Sb nuclei. A temperature stabilized α-Al_2O_3 crystal Bragg backscattering high-resolution monochromator with a relative energy resolution of 2×10^{-7} was introduced. As first spectroscopic applications the hyperfine parameters in Sb_2O_3, USb and DySb were determined. The energy of the nuclear transition in ^{121}Sb was measured to be 37.1298(2) keV, 40 times more precisely than reported before. The results open the field of nuclear resonance spectroscopy on antimony compounds taking advantage of the outstanding features of 3rd-generation synchrotron sources. Nuclear resonance scattering on Sb compounds at these sources allows element-specific dynamical studies on thermoelectric materials as well as studies on magnetism in micro- and nanometer dimensional systems like spintronic devices.

In this letter we report on the observation of nuclear resonant forward scattering (NFS) of synchrotron radiation (SR) from ^{121}Sb nuclei, and on studies in Sb compounds using this technique. The 37.1 keV nuclear resonance in ^{121}Sb can be used as a local probe for studying magnetic and electric structures in Sb compounds and their dynamics such as electron spin relaxation, diffusion, and vibrational dynamics. Antimony forms many compounds with interesting electronic and magnetic properties and is finding use in semiconductor technology for making infrared detectors, diodes and Hall-effect devices. Furthermore, antimony became recently of significant importance in the field of spintronics due to the giant magneto-resistance effect observed in MnSb [1]. Studies on the magnetic properties in such devices of micron dimension or smaller can be performed using NFS with a focused SR beam. Sb is also the last missing constituent for a complete picture of the element-specific vibrational density of states (DOS) in $EuFe_4Sb_{12}$ skutterudite, which shows interesting thermo-electrical properties [2]. Nuclear inelastic scattering (NIS) has already provided the independant DOS of the two other constituents, Fe and Eu. Classical Mössbauer spectroscopy was first applied for Sb compounds in 1965 with a ^{121}Sn radioactive source [3]. However the application of this technique is limited due to the insufficient brilliance of radioactive sources. Since 1985 new nuclear resonant techniques are in use, which use the brilliant synchrotron radiation as a source. The first successful nuclear resonant scattering experiment was reported on ^{57}Fe [4]. Since then the field of nuclear resonance spectroscopy with synchrotron radiation, namely the techniques of nuclear resonant forward scattering (NFS) [5] and nuclear resonant inelastic scattering (NIS) [6, 7], has been developed rapidly with a wide spread of applications in different fields of natural sciences covering magnetism, solid-state dynamics, phase transitions as well as biological and chemical studies [8, 9]. Due to the high brilliance of third-generation synchrotron radiation sources these techniques are unique in application to nanomagnetism and high-pressure physics where a high flux of resonant photons in very small sample volumina is mandatory [8]. ^{57}Fe is still the mostly studied Mössbauer isotope, but in paralell to a still growing field of studies on iron-containing systems, these spectroscopic techniques have been applied to ^{169}Tm (8.41 keV), ^{119}Sn (23.88 keV), ^{83}Kr (9.4 keV), ^{181}Ta (6.21 keV), ^{151}Eu (21.54 keV) [10], ^{161}Dy (25.651 keV) [11], ^{40}K (29.83 keV) [12], ^{129}I (27.75 keV) [13] and ^{149}Sm (22.49 keV) [14].

Essential for these techniques are the high-resolution monochromators (HRMs), allowing for filtering X-rays with meV spectral bandwidth from the broad spectrum of synchrotron radiation. For experiments, performed at transition energies lower than 30 keV, HRMs have been developed and are widely used (see reviews [15,16]). At higher energies HRMs are not available yet and therefore only the incoherent decay of the nuclear states excited by the synchrotron radiation was observed in ^{121}Sb (37.13 keV) [17] and ^{197}Au (77.35 keV) [18]. Recently, coherent resonant scattering from ^{61}Ni at 67.4 keV was observed using the nuclear lighthouse effect [19].

The design of high-resolution monochromators for hard X-rays is always a challenge. Bragg scattering from perfect crystals is used for this purpose. Bragg reflections are chosen with the intrinsic relative spectral width ϵ_{H} to be about of the required relative energy resolution $\Delta E/E$ of the monochromator [16]. For example, a monochromator for X-rays with an energy of $E = 37.1\,\mathrm{keV}$, matching the nuclear transition energy in ^{121}Sb, with an energy bandpass of $\Delta E = 1\,\mathrm{meV}$, requires a Bragg reflection with $\epsilon_{H} \simeq 3\times10^{-8}$. The intrinsic angular acceptance of Bragg reflections (and thus of the monochromator) is $\Delta\theta = \epsilon_{H}\tan\theta$. In our particular case it is very small unless the Bragg angle θ is close to 90°. In case of extreme backscattering geometry when $\theta \simeq 90^\circ$ the expression for $\Delta\theta$ becomes $\Delta\theta = 2\sqrt{\epsilon_{H}}$ [20], and in our particular case $\Delta\theta \simeq 3\times10^{-4}\,\mathrm{rad}$, which covers well the angular divergence of about 10 to 20 μrad of X-ray beams generated at the modern synchrotron radiation facilities. However, the extreme backscattering geometry requires Bragg reflection from atomic planes with a fixed inter-planar distance $d_{H} = hc/2E$ (which follows from Bragg's law $2d_{H}\sin\theta = hc/E$). The latter very often poses a problem, since for high-symmetry crystals like Si, which are mainly in use in X-ray optics due to their perfection, the series of d_{H} shows very broad gaps. In most cases simply no Bragg back-reflections for a certain fixed nuclear transition energy exist.

In case of photon energies below 30 keV this problem can be solved by using Bragg diffraction from multiple crystal arrangements in a dispersive configuration: first an asymmetric Bragg reflection decreases the angular width of the beam, then a second crystal, in back- but not extreme backscattering geometry with $70^\circ \leq \theta \leq 90^\circ$ providing high-energy resolution, determines the photon energy via θ [15, 16]. Another way to avoid this problem is to use crystals with lower symmetry, which have much smaller gaps in the spectrum of d_{H} than Si crystals [21]. Very attractive in this respect are sapphire (α-Al$_2$O$_3$) single crystals, which unlike Si have also high reflectivity for X-rays above 30 keV. The disadvantage is that the crystal perfection, which is mandatory to achieve a high-energy resolution, in general is not as high for sapphire as for silicon [16, 22]. The application of sapphire as a high-resolution monochromator was demonstrated in NFS studies on ^{161}Dy at 25.61 keV [23].

The lattice parameters of sapphire are known with good precision in the temperature range from 4 to 400 K [24, 25]. These data enable the evaluation of Bragg reflections and crystal temperatures for which the condition of exact Bragg backscattering $2d_{H} = hc/E$ is fulfilled for the desired photon energy E. Several reflections at different sapphire crystal

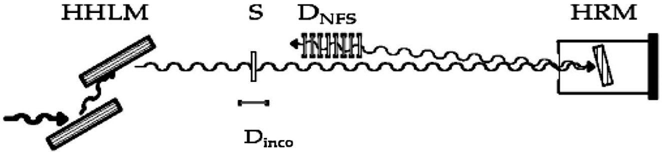

Fig. 1 – Schematic view of the experimental setup. HHLM: double-crystal Si(111) high-heat-load monochromator; S: sample containing ^{121}Sb; D_{inco}: X-ray Si APD detector used to adjust the HHLM to the 37.13keV nuclear resonance in ^{121}Sb; HRM: high-energy resolution monochromator consisting of a sapphire single crystal set into the position of almost exact Bragg backscattering from the $(15\ 13\ \overline{28}\ 14)$ atomic planes and maintained at constant temperature $T \simeq 146$ K in a cryostat; D_{NFS}: X-ray detector consisting of 12 semitransparent Si APDs and having an overall time resolution of 0.8ns.

temperatures can be used to build a high-resolution monochromator for 37.13 keV X-rays. According to [26] the nuclear transition energy of ^{121}Sb is 37.133(8) keV. Using this value and the data of [24,25] exact backscattering is expected, *e.g.*, with the $(15\ 13\ \overline{28}\ 14)$ Bragg reflection in the temperature range between 100 K to 200 K. This chosen reflection is the most favorable to construct a sapphire-based Bragg backscattering HRM for ^{121}Sb: first of all, in the low-temperature range the thermal expansion of sapphire is smaller and therefore the position of the peak reflectivity on the photon energy scale is not so sensitive to temperature changes, and second, it shows high reflectivity. The theoretical reflectivity is $R = 0.9$, the energy bandwidth of the reflection is $\Delta E = 0.42$ meV, $\epsilon_H = 1.1 \times 10^{-8}$, the angular acceptance is $\Delta\theta = 130\,\mu$rad (at exact normal incidence), and the extinction length is $L_{\text{e}} = 0.5$ mm. The variation of the peak reflectivity on the photon energy scale with temperature is -59 meV/K at $T \simeq 150$ K. The calculations were performed using the dynamical theory of X-ray diffraction with the sapphire crystal data [16]. In order to achieve the theoretical energy width of $\Delta E = 0.42$ meV and the maximum reflectivity of $R = 0.9$, a perfect sapphire single crystal with a thickness about $10L_{\text{e}} = 5$ mm is required. Good temperature stability and homogeneity across the crystal are also necessary. For example, a temperature gradient of 7 mK results in doubling the intrinsic energy width.

The experiments were performed at the nuclear resonance beamline ID18 of the European Synchrotron Radiation Facility (ESRF), Grenoble, France [27] during 16-bunch mode operation. A schematic view of the experimental setup is shown in fig. 1. A Si(111) high-heat-load monochromator (HHLM) provides radiation with about 5 eV bandwidth at 37.13 keV. Then the radiation passes through a sample (S) containing ^{121}Sb nuclei. A Si avalanche photo diode (APD) X-ray detector [28] is placed close to the sample off the direct beam (D_{inco}). The active Si wafer is $100\,\mu$m thick and has an area of $10 \times 10\,\text{mm}^2$. The time resolution of the detector is 0.6 ns. Since it is much smaller than the lifetime of the 37.13 keV nuclear excited state in ^{121}Sb of $\tau = 4.99(6)$ ns, measuring the delayed photons allows for detecting only those resonantly scattered from the 37.13 keV nuclear resonance in ^{121}Sb. The HHLM is tuned to the energy of the nuclear resonance in ^{121}Sb by detecting the maximum number of the delayed photons. After passing through the sample the beam arrives at the HRM —the sapphire crystal— located in a temperature-controlled liquid-nitrogen flux cryostat. A computer-driven temperature control permits to keep the temperature on the crystal stable within a few mK and to perform slow temperature scans [29]. The cryostat is mounted on a 4-circle goniometer enabling the angular crystal adjustment for backscattering from the $(15\ 13\ \overline{28}\ 14)$ planes.

The X-ray detector for nuclear forward scattering (D_{NFS}) is placed at a distance of $L = 12$ m from the sapphire crystal, and $l = 24$ mm above the incident beam. The X-ray detector is a stack of twelve Si APDs. A factor of two in its efficiency is gained by inclining

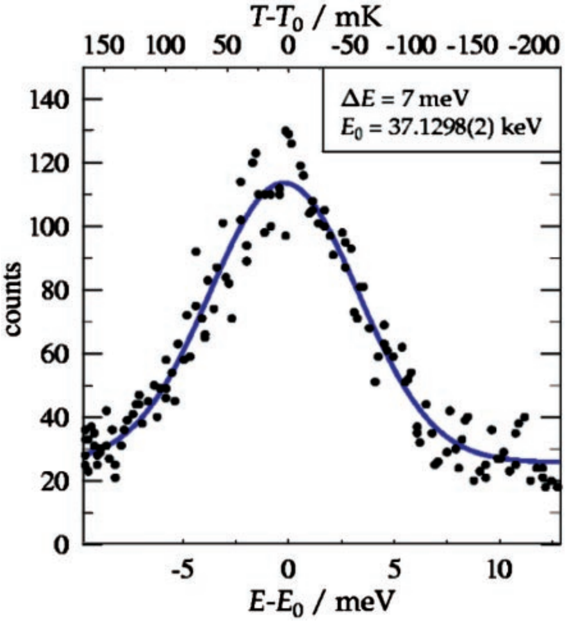

Fig. 2 – Energy dependence of the sapphire crystal reflectivity, the (15 13 $\overline{28}$ 14) Bragg back-reflection, measured by counting delayed 37.13 keV photons with the forward scattering detector (D_{NFS}) during a slow linear temperature scan; the counting time was 30 s per point. The peak reflectivity is achieved at a crystal temperature of $T_0 = 146.54(95)$ K, corresponding to the X-ray photon energy $E_0 = 37.1298(2)$ keV.

them by 60° and thus doubling the absorbing thickness of the diodes. The resulting efficiency of the detector at 37.1 keV is 37% and its overall time resolution is 0.8 ns. The latter allows for measuring the delayed emitted nuclear resonant quanta after a recovery time of some nanoseconds after each synchrotron radiation pulse. The detector (D_{NFS}) position defines the scattering angle and also the angle of incidence $\Theta = l/2L = \pi/2 - \theta = 1$ mrad ($\theta = 89.94°$) to the reflecting atomic planes (15 13 $\overline{28}$ 14) of the sapphire crystal. At this angle of incidence the intrinsic angular width of the reflection $\Delta\theta = \epsilon_H \tan\theta = 11.3\,\mu$rad just fits to the vertical angular divergence of the X-ray beam at ID18 of 12 μrad.

After the HHLM is tuned, the next step is to tune the HRM to the energy of the nuclear resonance. For this the sapphire crystal temperature is first set to a value where the energy of the reflected photons is within the HHLM bandwidth of 5.2 eV, which corresponds to a wide range of crystal temperatures of more than 80 K. Then the crystal temperature and thus the energy of the back-reflected photons from the sapphire crystal is adjusted to match the nuclear resonant energy of ^{121}Sb within the small bandwidth of the back-reflection by maximizing the count-rate of the delayed photons in the forward scattering detector (D_{NFS}).

Figure 2 shows the energy dependence of the sapphire crystal reflectivity, measured by the temperature dependence of X-ray photons back-reflected from the (15 13 $\overline{28}$ 14) atomic planes. Only delayed photons from a DySb sample are counted. The solid line represents a Gaussian fit to the reflection curve. The peak reflectivity is achieved at a crystal temperature of $T_0 = 146.54(95)$ K. According to the sapphire crystal lattice parameters data of [24] this corresponds to the photon energy $E_0 = 37.1298(2)$ keV. This value for the nuclear transition energy in ^{121}Sb is 40 times more precise than the value given in [26].

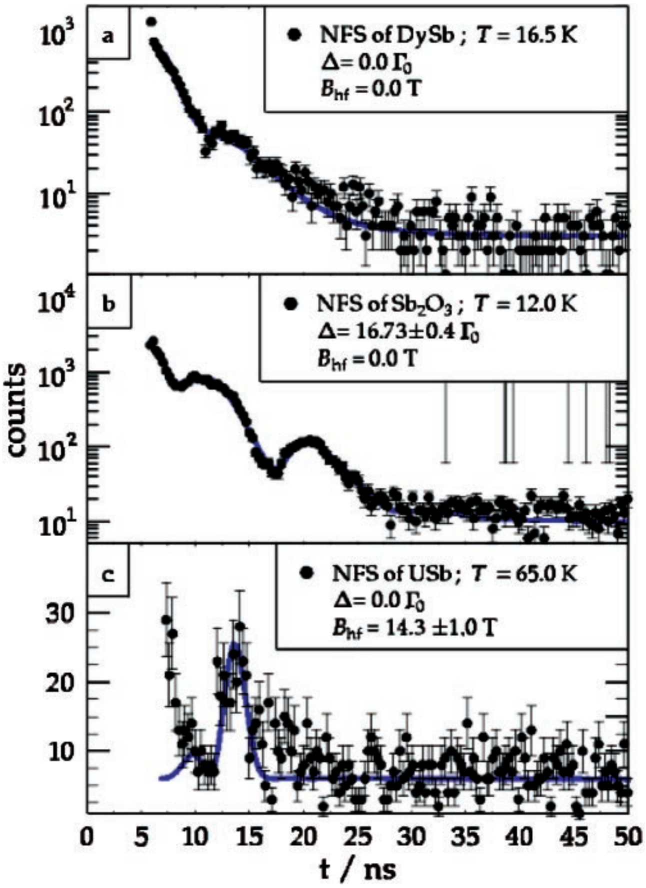

Fig. 3 – Time spectra of nuclear resonant forward scattering from ^{121}Sb in different compounds: DySb (a), Sb_2O_3 (b), and USb (c). The data collection time was about 2 h, 10 h and 4 h in 2048 channels, respectively. Three channels have been added subsequently resulting in a data collection time per point of 10.8 s, 53.5 s and 21.2 s, respectively. The background in the spectra is due to the noise of 12 APDs of about 0.25 counts per second. The solid lines represent fits within the framework of the NFS theory using the program MOTIF [30]. The quadrupole splitting parameter Δ is defined as $eV_{zz}Q$, with the elementary charge e, the main component of the electric field gradient V_{zz} and the quadrupole moment of the ground state Q. Δ is given in units of the natural linewidth of the 37.13 keV nuclear excited state $\Gamma_0 = \hbar/\tau = 132$ neV. Note: the axis of counts of the USb data are linearly scaled.

The width of the energy distribution is 7 meV. The relative energy resolution of the sapphire monochromator is thus 2×10^{-7}. The measured energy width is about 15 times larger than the theoretical value for a perfect crystal. This is first of all due to the presence of some dislocations in the sapphire crystal. A high-quality crystal from Crystal Systems Inc. has been chosen among others using X-ray topography [22]. The measured dislocation density was about $10^2/\text{cm}^2$. A temperature gradient of 0.1 K could also explain a broadening of 7 meV. Despite the broadening, the HRM provides a sufficiently narrow bandwidth and thus fair low load on the X-ray detector and timing electronics enabling us to perform measurements of the time spectra of nuclear forward scattering.

To measure time spectra the sapphire crystal is stabilized at $T_0 = 146.54(95)$ K to provide the maximum count-rate of delayed photons. Time spectra of NFS in three Sb-containing compounds (natural abundance of the ^{121}Sb isotope = 57.25%) were measured. The nuclear transition in ^{121}Sb takes place between the ground and excited states with spin and parity 5/2+ and 7/2+, respectively. A magnetic dipole ($M1$) radiation transition in 18 channels between the hyperfine sub-levels is allowed. The natural linewidth of the 37.13 keV nuclear excited state $\Gamma_0 = \hbar/\tau = 131.6\,\text{neV}$, which is defined by the lifetime $\tau = 4.99\,\text{ns}$ of the 37.13 keV excited state. Figure 3 shows the measured time spectra of NFS in DySb (a), Sb_2O_3 (b), USb (c), respectively. The solid lines represent fit results achieved with the program MOTIF within the framework of the NFS theory [30].

The time spectrum in DySb was measured at 16.5 K, *i.e.*, above the Néel temperature of 9.5 K. DySb has a cubic NaCl-type crystal structure, where the site symmetry of the Sb atoms is $m\bar{3}m$. Thus, no splitting of the levels in the ground or excited state due to magnetic-dipole or electric-quadrupole interaction is expected. The time spectrum calculated accordingly is shown as a solid line in fig. 3(a). It shows one special feature, a Bessel thickness oscillation, which is due to a large effective resonant absorbing thickness of the sample and fits fairly well to the experimental spectrum.

The Sb_2O_3 sample was ascertained to be of cubic crystal structure using powder X-ray diffraction. The point symmetry $.3m$ of the Sb atoms indicates that they occupy sites of axial symmetry. The fit to the 12 K NFS spectrum (fig. 3b) is obtained by assuming a pure axial electric-quadrupole interaction. The quadrupole splitting parameter as determined from the fit is $\Delta = (16.7 \pm 0.4)\ \Gamma_0$. It agrees well within the errors with the value $\Delta = (17.2 \pm 0.6)\ \Gamma_0$ reported earlier based on Mössbauer spectroscopy measurements [31, 32].

Figure 3c shows the time spectrum of USb measured in the magnetically ordered state at 65 K (Néel temperature 213 K). The data can be fitted assuming that the ^{121}Sb nuclei experience a magnetic hyperfine field $B_{\text{hf}} = (14.3 \pm 1.0)$ T. This transferred field is due to the polarization of the Sb 5*sp* electrons by the magnetic moment of uranium [33]. The quadrupole interaction is zero due to the NaCl-type structure of USb at 65 K.

In conclusion, we performed nuclear resonant forward scattering spectroscopy with synchrotron radiation at the ^{121}Sb transition at 37.13 keV in different Sb-containing compounds: DySb, Sb_2O_3 and USb. The electric-quadrupole splitting and hyperfine magnetic field at the nuclear site were determined. Hyperfine spectroscopy studies become possible thanks to the developed high-resolution sapphire Bragg backscattering monochromator for 37.1 keV photons. The achieved relative energy resolution is 2×10^{-7}. The bandpass of the monochromator is 7 meV. The energy of the nuclear transition in ^{121}Sb was determined to be 37.1298(2) keV. The experiment shows that nuclear resonant spectroscopy of ^{121}Sb using synchrotron radiation is accessible using sapphire Bragg backscattering monochromators. Within the variety of applications opened by extending the field of nuclear resonant scattering of SR (NFS and NIS) to the ^{121}Sb isotope we mention two examples of actual interest: spintronic devices based on MnSb and thermoelectric devices based on filled skutterudites.

* * *

We are grateful to Prof. E. Gerdau and K. Geske for their effort in the development of the APD stack detector, to M. Lucht for providing the temperature control software and participation in the design of the liquid-nitrogen cryostat and to C. P. Chandra for providing the sapphire crystal.

REFERENCES

[1] Akinaga H., *Semicond. Sci. Technol.*, **17** (2002) 322.

[2] Hermann R. P., Jin R., Schweika W., Grandjean F., Mandrus D., Sales B. C. and Long G. J., *Phys. Rev. Lett.*, **90** (2003) 135505.

[3] SNYDER R. E. and BEARD G. B., *Phys. Lett.*, **15** (1965) 264.
[4] GERDAU E., RÜFFER R., WINKLER H., TOLKSDORF W., KLAGES C. P. and HANNON J. P., *Phys. Rev. Lett.*, **54** (1985) 835.
[5] HASTINGS J. B., SIDDONS D. P., VAN BÜRCK U., HOLLATZ R. and BERGMANN U., *Phys. Rev. Lett.*, **66** (1991) 770.
[6] SETO M., YODA Y., KIKUTA S., ZHANG X. W. and ANDO M., *Phys. Rev. Lett.*, **74** (1995) 3828.
[7] STURHAHN W., TOELLNER T. S., ALP E. E., ZHANG X., ANDO M., YODA Y., KIKUTA S., SETO M., KIMBALL C. W. and DABROWSKI B., *Phys. Rev. Lett.*, **74** (1995) 3832.
[8] DE WAARD H. and GERDAU E. (Editors), *Nuclear Resonant Scattering of Synchrotron Radiation, Hyperfine Interact.*, **123-125** (1999/2000).
[9] RÖHLSBERGER R., *Nuclear Solid State Physics with Synchrotron Radiation, Springer Tracts Modern Phys.*, Vol. **208** (Springer Verlag, Berlin) 2004.
[10] LEUPOLD O., CHUMAKOV A. I., ALP E. E., STURHAHN W. and BARON A., *Hyperfine Interact.*, **123/124** (1999) 611.
[11] CHUMAKOV A. I., RÜFFER R., LEUPOLD O., BARLA A., THIESS H., GIL G. M., ALBERTO H. V., VILAO R. C., AYNS DE CAMPOS N., KOHN V. G., GERKEN M. and LUCHT M., *Phys. Rev. B*, **63** (2001) 172301.
[12] SETO M., KITAO S., KOBAYASHI Y., HARUKI R., MITSUI T., YODA Y., ZHANG X. W., KISHIMOTO S. and MAEDA Y., *Hyperfine Interact.*, **141** (2002) 99.
[13] KITAO S., private communication.
[14] BARLA A., SANCHEZ J. P., HAGA Y., LAPERTOT G., DOYLE B. P., LEUPOLD O., RÜFFER R., ABD-ELMEGUID M. M., LENGSDORF R. and FLOUQUET J., *Phys. Rev. Lett.*, **92** (2004) 066401.
[15] TOELLNER T. S., *Hyperfine Interact.*, **125** (2000) 3.
[16] SHVYD'KO YU. V., *X-Ray Optics, Springer Ser. Opt. Sci.*, Vol. **98** (Springer Verlag, Berlin) 2004.
[17] KITAO S., MITSUI T. and SETO M., *J. Phys. Soc. Jpn.*, **69** (2000) 683.
[18] KISHIMOTO S., YODA Y., SETO M., KOBAYASHI Y., KITAO S., HARUKI R., KAWAUCHI T., FUKUTANI K. and OKANO T., *Phys. Rev. Lett.*, **85** (2000) 1831.
[19] ROTH T., LEUPOLD O., WILLE H.-C., RÜFFER R., QUAST K. W., RÖHLSBERGER R. and BURKEL E., *Phys. Rev. B*, **71** (2005) 140401(R).
[20] KOHRA K. and MATSUSITA T., *Z. Naturforsch. A*, **27** (1972) 484.
[21] SHVYD'KO YU. V. and GERDAU E., *Hyperfine Interact.*, **123/124** (1999) 741.
[22] CHEN W. M., MCNALLY P. J., SHVYD'KO YU. V., TUOMI T., LERCHE M., DANILEWSKY A. N., KANATHARANA J., LOWNEY D., O'HARE M., KNUUTTILA L., RIIKONEN J. and RANTAMÄKI R., *Phys. Status Solidi a*, **186** (2001) 365.
[23] SHVYD'KO YU. V., GERKEN M., FRANZ H., LUCHT M. and GERDAU E., *Europhys. Lett.*, **56** (2001) 309.
[24] LUCHT M., LERCHE M., WILLE H.-C., SHVYD'KO YU. V., RÜTER H. D., GERDAU E. and BECKER P., *J. Appl. Cryst.*, **36** (2003) 1075.
[25] SHVYD'KO YU. V., LUCHT M., GERDAU E., LERCHE M., ALP E. E., STURHAHN W., SUTTER J. and TOELLNER T. S., *J. Synchrotron Radiat.*, **9** (2002) 17.
[26] TAMURA T., *Nucl. Data Sheets*, **90** (2000) 107.
[27] RÜFFER R. and CHUMAKOV A. I., *Hyperfine Interact.*, **97/98** (1996) 589.
[28] BARON A. Q. R., *Hyperfine Interact.*, **125** (2000) 29.
[29] LUCHT M., Diploma Thesis, University of Hamburg (1998).
[30] SHVYD'KO YU. V., *Phys. Rev. B*, **59** (1999) 9132.
[31] SVANE A., *Phys. Rev. B*, **68** (2003) 064422.
[32] RUBY S. L., KALVIUS M., BEARD G. B. and SNYDER R. E., *Phys. Rev.*, **159** (1967) 239.
[33] SANCHEZ J. P., SPIRLET J. C., REBIZANT J. and VOGT O., *J. Magn. & Magn. Mater.*, **63-64** (1987) 139.